

# Design, Synthesis, $^{99m}\text{Tc}$ Labeling, and Biological Evaluation of a Novel Pyrrolizine Derivative as Potential Anti-Inflammatory Agent

K. M. Attallah<sup>\*a,b</sup>, A. M. Gouda<sup>c,d</sup>, I. T. Ibrahim<sup>b</sup>, and L. Abouzeid<sup>e</sup>

<sup>a</sup> Department of Pharmaceutics, College of Pharmacy, Umm Al-Qura University, Makkah, 21955 Saudi Arabia

<sup>b</sup> Labeled Compounds Department, Hot Laboratories Center, Atomic Energy Authority, P.O. Box 13759, Cairo, Egypt

<sup>c</sup> Department of Medicinal Chemistry, Faculty of Pharmacy, Beni-Suef University, Beni-Suef, 62514 Egypt

<sup>d</sup> Department of Pharmaceutical Chemistry, College of Pharmacy, Umm Al-Qura University, Makkah, 21955 Saudi Arabia

<sup>e</sup> Department of Pharmaceutical Organic Chemistry, Faculty of Pharmacy, Mansoura University, 35516 Egypt

\*e-mail: Kmhassan@uqu.edu.sa

Received March 20, 2017

**Abstract**—The design and synthesis of ethyl 4-(6-amino-7-cyano-2,3-dihydro-1*H*-pyrrolizine-5-carboxamido)-benzoate (KH16) were discussed, and its structure was determined. The anti-inflammatory activity of a new compound was evaluated using in vitro cyclooxygenase (COX) inhibitory assay. KH16 exhibits higher selectivity to COX-2 than to COX-1 with the selectivity index of 3.46. KH16 was labeled with  $^{99m}\text{Tc}$  with the maximum radiochemical yield of  $^{99m}\text{Tc}$ -KH16 of  $90.5 \pm 1.5\%$ . Biodistribution of  $^{99m}\text{Tc}$ -KH16 in normal, infected, and inflamed mice was studied. The uptake in inflamed muscle was higher than that in normal muscle throughout the examined time interval. This work is a step ahead in the direction of using pyrrolizine derivatives for site-specific delivery to the inflamed tissue.

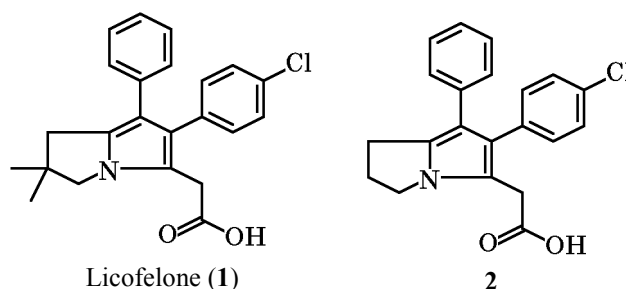
**Keywords:** pyrrolizine, anti-inflammatory drugs, COX, technetium-99m, inflammation, infection

**DOI:** 10.1134/S10663622170600121

Nonsteroid anti-inflammatory drugs (NSAIDs) are among the most widely used drugs in the world [1]. The wide use of NSAIDs in treatment of inflammations, pain, and hyperthermia is often accompanied by a wide range of side effects [2, 3], of which gastrointestinal erosions and bleeding are the most common [4]. Most of NSAIDs exert their actions through cyclooxygenase (COX) inhibition [5]. Along with being a vital key element in the normal physiological function of the stomach, COX enzymes plays a crucial role in inflammation response and cell proliferation [6, 7].

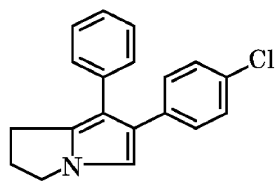
Several pyrrolizine-based anti-inflammatory agents have been reported [8–16]. Of these pyrrolizines, licofelone **1** displayed anti-inflammatory, analgesic, and antipyretic activities mediated by COX/5-LOX inhibi-

tion, with little or no damage of the gastric mucosa [9, 10]. The structure–activity relationship for licofelone showed that the removal of the 2,2-dimethyl groups and removal/masking of the free carboxy group resulted in active anti-inflammatory agents (compounds **2–5** [11–14];  $\text{IC}_{50}$  is the half-maximum inhibition concentration,  $\mu\text{M}$ , and IP is the inhibition percent).

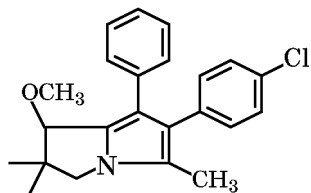


$\text{IC}_{50} = 0.21$  (COX),  $0.18$  (5-LOX)  $\text{IC}_{50} = 2$  (COX),  $1.6$  (5-LOX)

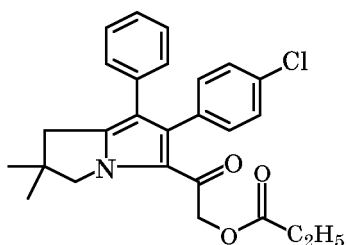
<sup>1</sup> The text was submitted by the authors in English.



3

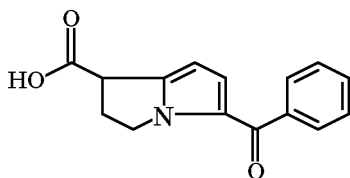
IP = 10% (COX-1),  $\text{IC}_{50}$  = 3.6 (COX-2)

4

 $\text{IC}_{50}$  = 0.5 (COX-1), 7.5 (COX-2)

5

IP &gt; 20% (COX-1), &gt; 10% (COX-2)



(R,S)-Ketorolac (6)

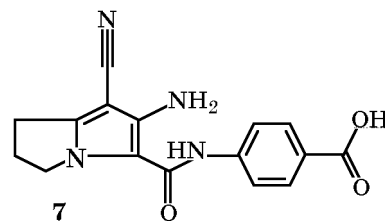
 $\text{IC}_{50}$  = 1.23 (hCOX-1), 3.50 (hCOX-2)

Ketorolac **6** displayed potent anti-inflammatory and analgesic activity mediated by inhibition of COX enzymes [15]. The (*S*) enantiomer of ketorolac showed 60 times more potent anti-inflammatory activity than the (*R*) enantiomer did [16].

The conventional anatomical imaging techniques such as computerized tomography (CT), radiology, and nuclear magnetic resonance (NMR) were unable to differentiate between inflammatory and infectious processes [17]. The development of  $^{99m}\text{Tc}$ -based radiopharmaceutical provides a better tool to differentiate between inflammatory and infectious lesions [18]. The  $^{99m}\text{Tc}$ -labeled selective and nonselective NSAIDs have been used in inflammation imaging [19, 20]. On the other hand,  $^{99m}\text{Tc}$ -labeled antibacterial agents were used in imaging of infection sites [21, 22].

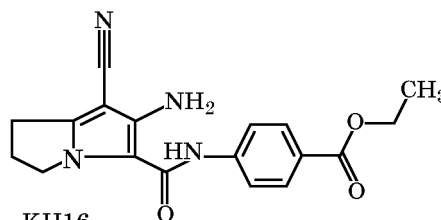
Previously we have reported compound **7** as an analgesic anti-inflammatory agent which displayed near-

ly 60% of the anti-inflammatory activity of ketorolac [23]. In this work, a potential anti-inflammatory agent, KH16, was designed and synthesized by masking the free carboxy group in compound **7**.



7

↓Masking of COOH group



KH16

The upregulated COX-2 in inflammation and cancer provides useful target in designing COX-2 selective inhibitors and in imaging of inflammation and cancer using radiolabeled COX-2 inhibitors. This study was also aimed at investigating the mechanism of action of KH16, its tagging with  $^{99m}\text{Tc}$ , the factors affecting the labeling yield, tissue localization, and efficacy of the compound as anti-inflammatory agent in model septic and aseptic inflammations.

## EXPERIMENTAL

### Chemicals and Instruments

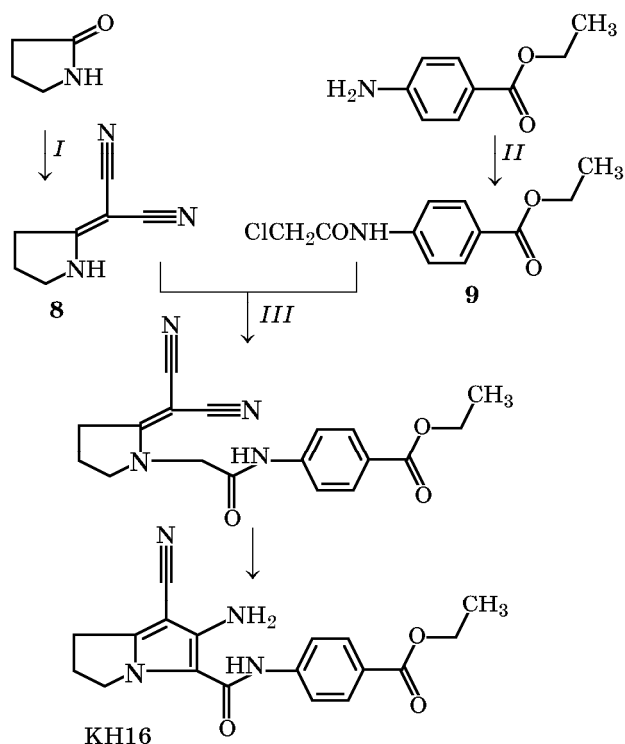
Chemical reagents and solvents were obtained from Sigma-Aldrich (commercial sources in Saudi Arabia). Solvents were dried by standard methods when necessary. The melting points (mp) were uncorrected and were determined by the open capillary tube method using IA 9100MK-Digital Melting Point Apparatus. Microanalyses were carried out at the Microanalytical Center, Faculty of Science, Cairo University. The IR spectra were taken with a Bruker Tensor 37 spectrophotometer using KBr pellets. The  $^1\text{H}$  NMR spectra were recorded on a Bruker Avance II spectrometer at the faculty of pharmacy, Umm Al-Qura University at 500 MHz in  $\text{CDCl}_3$ . The chemical shifts are presented on the  $\delta$  scale using the residual solvent signal as internal reference, and the  $J$  values are given in Hz. The  $^{13}\text{C}$  NMR and DEPT135 spectra were recorded on the same spectrometer at 125 MHz. The mass spectra were

recorded on a Shimadzu GCMS QP5050A spectrometer at 70 eV (EI) at the Regional Center for Mycology and Biotechnology, Al-Azhar University. Thin layer chromatography was done using Macherey–Nagel AlugramSil G/UV254 silica gel plates and benzene–ethanol (9.5 : 0.5) as the eluting system.

### Synthesis of Organic Compounds

**Preparation of 2-pyrrolidin-2-ylidenemalononitrile 8.** Compound **8** was synthesized as described previously [24]. A solution of 2-pyrrolidinone (5 g, 58.8 mmol) in dry benzene (15 mL) was treated with dimethyl sulfate (7.4 g, 58.8 mmol, see scheme). The reaction mixture was refluxed for 3 h and then allowed to cool. A concentrated NaOH solution (3 mL, 600 g L<sup>-1</sup>) was added dropwise. The organic phase was separated, dried over anhydrous sodium sulfate, and filtered. Malononitrile (2.5 g, 38.2 mmol) was added to the benzene solution, whereby white crystals were formed. The crystals were collected, dried (yield 5.9 g, 75%), and recrystallized from ethanol, mp 159–161°C (published data: 158–159°C).

**Preparation of ethyl 4-(2-chloroacetamido)benzoate 9.** Compound **9** was synthesized by the proce-



Scheme of the synthesis of KH16. (I) (CH<sub>3</sub>)<sub>2</sub>SO<sub>4</sub>, benzene, CH<sub>2</sub>(CN)<sub>2</sub>; (II) ClCH<sub>2</sub>COCl, glacial acetic acid, CH<sub>3</sub>COONa; (III) acetone, K<sub>2</sub>CO<sub>3</sub>, reflux, 24 h.

cedure described in [25] with some modifications. Ethyl 4-aminobenzoate (54 mmol) was reacted with chloroacetyl chloride in glacial acetic acid. Saturated aqueous solution of sodium acetate (3 mL) was added dropwise after complete addition of chloroacetyl chloride. The heavy precipitate formed was filtered off, washed with water, and recrystallized from ethanol.

**Preparation of ethyl 4-(6-amino-7-cyano-2,3-dihydro-1H-pyrrolizine-5-carboxamido)benzoate (KH16).** A mixture of **9** (1.81 g, 7.5 mmol), **8** (1 g, 7.5 mmol), and anhydrous K<sub>2</sub>CO<sub>3</sub> (1.04 g, 7.5 mmol) in dry acetone (50 mL) was stirred for 24 h under reflux. The reaction mixture was filtered while hot, concentrated, and left to cool. The crystals formed were collected, dried, and recrystallized from ethanol–acetone mixture. Compound KH16 was obtained as yellowish white crystals, mp 228–230°C, yield 62%. IR, ν, cm<sup>-1</sup>: 3448, 3340, 3300 (NH), 3038 (C–H aromatic), 2927 (C–H aliphatic), 2210 (CN), 1699, 1638 (C=O). <sup>1</sup>H NMR (CDCl<sub>3</sub>, 500 MHz), δ, ppm: 1.42 t (3H, *J* = 7.0 Hz, CH<sub>3</sub>), 2.56 m (2H, CH<sub>2</sub>-2), 3.02 t (2H, *J* = 7.5 Hz, CH<sub>2</sub>-1), 3.60 s (2H, NH<sub>2</sub>), 4.37–4.44 m (4H, OCH<sub>2</sub> + CH<sub>2</sub>-3), 7.68 d (2H, *J* = 10 Hz, aromatic CH-2', CH-6'), 8.05 d (2H, *J* = 10 Hz, aromatic CH-3', CH-5'), 9.84 s (H, NH). <sup>13</sup>C NMR (CDCl<sub>3</sub>), δ, ppm: 14.37 (CH<sub>3</sub>), 24.79 (CH<sub>2</sub>-1), 25.43 (CH<sub>2</sub>-2), 49.75 (CH<sub>2</sub>-3), 60.81 (OCH<sub>3</sub>), 83.58 (C-7), 114.25 (C≡N), 114.59 (phenyl C-4), 118.71 (phenyl C-2 + C-6), 125.56 (C-5), 130.85 (phenyl C-3 + C-5), 137.66 (C-7a), 142.35 (phenyl C-1), 145.58 (C-6), 158.70 (CONH), 166.19 (COO). MS (EI), *m/z* (*I*, %) 339 (M<sup>+</sup> + 1, 3), 338 (M<sup>+</sup>, 16), 324 (2), 293 (2), 265 (1), 237 (1), 174 (100), 146 (41), 120 (21), 105 (3), 92 (27), 77 (2). Analytical data: Calculated for C<sub>18</sub>H<sub>18</sub>N<sub>4</sub>O<sub>3</sub> (*M* = 338.36), %: C 63.89, H 5.36, N 6.56. Found, %: C 63.47, H 5.20, N 16.72.

### Pharmacological Screening

**In vitro COX-1/2 inhibitory assay.** The ability of the tested compound KH16 to inhibit COX-1 (ovine) and COX-2 (human recombinant) was measured using COX colorimetric inhibitor screening assay kit (Cayman Chemical, Ann Arbor, MI, the United States, catalog no. 560 131) according to the manufacturer's instructions. The procedure was described previously [26].

### Preparation and Analysis of the Labeled Compound, Evaluation of Its Stability

**Labeling process.** The required amount of the ligand (KH16) was transferred to a clean evacuated

10-mL penicillin vial and then was dissolved in 1 mL of DMSO. The vial was closed under positive pressure of nitrogen gas, and then the required amount of tin(II) chloride was added. 1 mL of  $^{99m}\text{Tc}$  eluate (2 mCi mL<sup>-1</sup>) was added to the above mixture, and pH 5 was adjusted with a few drops of phosphate buffer (0.5 M). The reaction volume was completed to 2.2 mL with normal saline and incubated for the recommended time before assay of the  $^{99m}\text{Tc}$ -ligand complex.

**Paper chromatography.**  $^{99m}\text{Tc}$ -KH16 was separated from free pertechnetate and reduced hydrolyzed species using paper chromatography with two developing systems. Acetone was used to determine free pertechnetate, which moved to the top of the chromatogram ( $R_f = 1$ ), whereas reduced hydrolyzed species and  $^{99m}\text{Tc}$ -KH16 remained at the point of spotting ( $R_f = 0$ ). 5 N NaOH was used as the mobile phase to determine reduced hydrolyzed species, which remained at the origin ( $R_f = 0$ ), whereas free pertechnetate and  $^{99m}\text{Tc}$ -KH16 moved with the solvent front ( $R_f = 1$ ). The radiochemical yield was determined by subtracting the relative content of free pertechnetate and reduced hydrolyzed species from 100% [27]. The radiochemical yield is the mean value of three experiments.

**Electrophoresis** was done with a EC-3000 p-series (E.C. Apparatus Corporation) programmable power and chamber supply units using cellulose acetate strips. The strips were moistened with 0.05 M phosphate buffer (pH  $7.2 \pm 0.2$ ) and then were introduced into the chamber. The  $^{99m}\text{Tc}$ -KH16 solution was passed through a Millipore filter (0.22  $\mu\text{m}$ ) to separate colloids, if present. Samples (5  $\mu\text{L}$ ) were applied at a distance of 10 cm from the cathode. The experiment was performed for 1.5 h at a voltage of 300 V. The strips were dried, cut into 1-cm segments, and counted with a well-type  $\gamma$ -scintillation counter. The radiochemical yield was calculated as the ratio of the radioactivity of the labeled product to the total radioactivity [28].

**HPLC analysis** was done by injecting a 10  $\mu\text{L}$  sample after filtration through a 0.22- $\mu\text{m}$  Millipore filter into the column (RP-18,  $300 \times 3.9$  mm, Alpha bond). We used a UV detector (SPD-6A) adjusted to the 260 nm wavelength. The column was eluted with a mixture of 60% acetonitrile and 40% water. The flow rate was 1 mL min<sup>-1</sup>. Fractions of 1 mL volume were collected separately using a fraction collector (up to 30 fractions) and counted using a well-type NaI(Tl) detector connected to a single-channel analyzer.

**In vitro stability in saline.** A solution of  $^{99m}\text{Tc}$ -

KH16 (0.1 mL) in 0.9% NaCl, prepared as described above, was diluted with 0.9% NaCl to a volume of 2 mL and incubated at  $37 \pm 1^\circ\text{C}$ . PC was performed at different time intervals (1, 2, 4, 6 and 8 h). The degree of degradation was judged from a decrease in the percentage of  $^{99m}\text{Tc}$ -KH16.

**In vitro stability in human serum** was studied similarly, except that human serum (1.9 mL) was used instead of 0.9% NaCl for diluting the  $^{99m}\text{Tc}$ -KH16 solution.

#### *Biological Characteristics of $^{99m}\text{Tc}$ -KH16*

The study was approved by the animal ethics committee, Labeled Compounds Department, and was in accordance with the guidelines set out by the Egyptian Atomic Energy Authority.

#### **Induction of septic and aseptic inflammation.**

Three groups of Swiss Albino mice (weighing 25 g), each of 25 mice, were used. In the first group, septic inflammation was induced in the right thigh of each mouse by intramuscular injection of  $1 \times 10^5$  *E. coli* cells. Inflammation developed within 7 days [29]. In the second group, aseptic inflammation was induced in the right thigh of each mouse by intramuscular injection of sterile turpentine oil (0.1 mL/mouse) [30]. Two days later, swelling appeared [31]. The third group consisted of normal mice.

**In vivo biodistribution.** Each animal was injected with 100  $\mu\text{L}$  of a solution containing 3.7 MBq (100  $\mu\text{Ci}$ , 0.148  $\mu\text{mol}$ ) of  $^{99m}\text{Tc}$ -KH16 via the tail vein. The mice were kept in metabolic cages for the required time, weighed, anaesthetized with chloroform, and sacrificed by cervical dislocation at 5, 15, 30, 60, and 120 min post injection. Five mice were taken for each time point. Organs or tissues of interest were removed, washed with saline, and weighed; their activity was measured in a shielded well-type  $\gamma$ -scintillation counter using a sample containing 1% of the injected dose as a reference. The results were calculated as percent of the injected dose per gram of tissue or organ (% ID/g). The weights of blood, bones, and muscles were assumed to be 7, 10 and 40% of the total body weight, respectively [32]. The ratio of the uptake in the infected (inflamed) thigh muscle to that in normal (control) thigh muscle was also calculated [33].

#### *Docking Study*

Comparative molecular modeling studies of the binding mode of compound KH16 in both COX-1 and

**Table 1.** In vitro inhibition of COX-1/2 enzymes with KH16

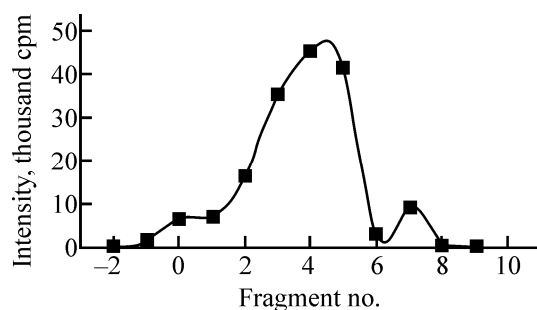
Compound	COX-1	COX-2	SI
	IC <sub>50</sub> , μM		
KH16	5.33	1.54	3.46
Indomethacin	0.73	32.6	0.02
Celecoxib	15.6	0.32	48.75

COX-2 pockets were performed to delineate the interaction features. The starting coordinates of the X-ray crystal structure of the COX-2 enzyme in the complex with SC-558 (1CX2) and COX-1 (PDB code 2OYE) were obtained from RCSB protein databank (Brookhaven National Laboratory) [34, 35]. The hydrogen atoms were added, and the enzyme structure was subjected to the refinement protocol in which the constraints on the enzyme were gradually removed and minimized until the rms gradient became 0.01 kcal mol<sup>-1</sup> Å<sup>-1</sup>. The energy minimization was carried out by the method of molecular mechanics with AMBER force field.

The newly designed compound KH16 was constructed from fragment libraries using ChemDraw program. The partial atomic charges for each analog were calculated by AM1 semiempirical method implemented in MOE program package. The docking was carried out on both COX-1 and COX-2 enzyme. The lowest-energy conformer (global minimum) was prepositioned using the crystal structure of SC-558 ligand as a template. Compound KH16 was optimally docked in the enzyme binding pocket.

#### Statistical Analysis

The results are expressed as mean ± SD for at least three experiments in the case of labeling procedures and five experiments in the case of biological study. For all analyses, the significance level  $P < 0.05$  was set, and unpaired Student's *t*-test was used.

**Fig. 1.** Electrophoretic pattern of <sup>99m</sup>Tc-KH16.

## RESULTS AND DISCUSSION

### Synthesis and Properties of KH16

The KH16 synthesis procedure is described above. In the IR spectrum of KH16, the absorption bands of the geminal CN groups disappear, and a single CN stretching band appears at 2210 cm<sup>-1</sup>. In addition, NH stretching bands appear at 3448, 3340, and 3300 cm<sup>-1</sup>, and a carbonyl absorption band appears at 1699 cm<sup>-1</sup>. In the <sup>1</sup>H NMR spectrum of KH16, a singlet at 1.42 ppm belongs to CH<sub>3</sub> protons; a singlet at 3.60 ppm, to NH<sub>2</sub> protons; two doublets at 7.68 and 8.04 ppm, to the *p*-substituted phenyl ring; and a singlet at 9.84 ppm, to the amide proton. The <sup>13</sup>C NMR spectrum consists of 16 signals in the range 14.37–166.19 ppm, of which the highest-field signal belongs to the CH<sub>3</sub> group (14.37 ppm), and the lowest-field signals, to the carbonyl groups (158.70 and 166.19 ppm). The DEPT-135 spectrum was used to differentiate between different types of carbon atoms. The mass spectrum of KH16 contains the molecular ion peak at *m/z* 338 with the relative abundance of 16%.

**In vitro COX inhibitory assay.** For the majority of NSAIDs, the COX inhibition is the main mechanism of action [36]. The ability of KH16 to inhibit COX enzymes was compared to that of indomethacin (nonselective COX inhibitor) and celecoxib (selective COX-2 inhibitor). The results were expressed in terms of IC<sub>50</sub> values and COX-1/COX-2 selectivity index (SI) (Table 1). It was noteworthy that KH16 has certain COX-2 selectivity over COX-1 with the selectivity index of 3.46.

### Analysis of Labeled KH16

**Electrophoresis** revealed that <sup>99m</sup>Tc-KH16 moved toward the anode (suggesting anionic nature of the complex), and <sup>99m</sup>TcO<sub>4</sub><sup>-</sup> moved toward the anode to a considerably longer distance (Fig. 1).

**HPLC analysis** (Fig. 2) showed that the retention time of <sup>99m</sup>Tc-KH16 was approximately 16 min, whereas the retention time of KH16 was approximately 14 min (UV detector).

### Factors Influencing the Labeling Yield

**Tin chloride content.** The majority of <sup>99m</sup>Tc-radiopharmaceuticals are prepared using SnCl<sub>2</sub>·2H<sub>2</sub>O [Sn(II)] for reducing <sup>99m</sup>Tc from heptavalent to lower valence state, which facilitates its chelation by com-

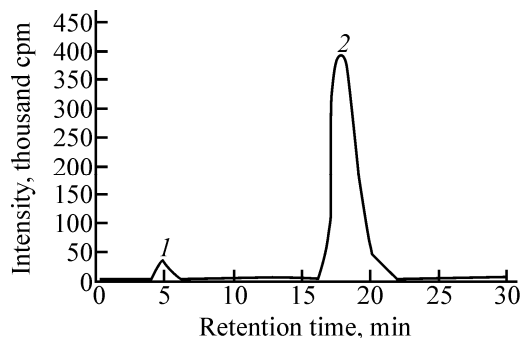


**Fig. 2.** HPLC of (1) free  $^{99m}\text{TcO}_4^-$  and (2)  $^{99m}\text{Tc}$ -KH16.

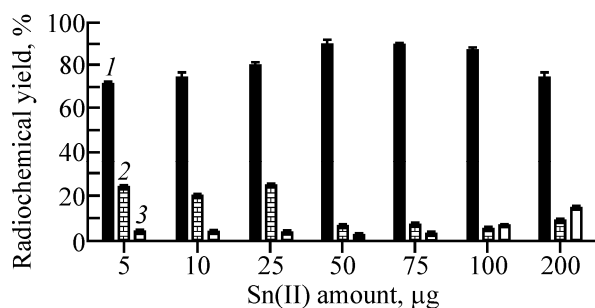


**Fig. 3.** Influence of the Sn(II) content on the radiochemical yield of  $^{99m}\text{Tc}$ -KH16. Conditions: 1 mg of KH16,  $20\text{mCi mL}^{-1}$   $^{99m}\text{TcO}_4^-$  solution, pH 5, room temperature, 10 min. (1)  $^{99m}\text{Tc}$ -KH16, (2) free pertechnetate, and (3) colloid; the same for Figs. 4–6.

pounds of diagnostic importance. The effect of tin chloride as a reducing agent on the labeling of KH16 with  $^{99m}\text{Tc}$  is illustrated in Fig. 3. As can be seen, the radiochemical yield significantly increased as the Sn(II) amount was increased from 5 (0.042  $\mu\text{mol}$ ) to 50  $\mu\text{g}$  (0.421  $\mu\text{mol}$ ), reaching a maximum of 90.3%. Further increase in the Sn(II) amount above 50  $\mu\text{g}$  leads to a decrease in the labeling yield (75.5% at 200  $\mu\text{g}$ , 1.684  $\mu\text{mol}$ ) owing to colloid formation (15.1%).

**Substrate amount.** The influence of the KH16 amount on the labeling yield was studied with the Sn(II) amount fixed at 50  $\mu\text{g}$ . The results are shown in Fig. 4. Increasing the amount of KH16 was accompanied by a significant increase in the labeling yield: from 81.5% at 200  $\mu\text{g}$  (0.59  $\mu\text{mol}$ ) to 90.5% at 1 mg (2.95  $\mu\text{mol}$ ), which is associated with the presence of a minimum limit for the volume used [37]. The 1-mg amount of KH16 is optimum. At larger amounts of KH16, the labeling yield decreases because of increased formation of colloids and, probably, increased generation of free radicals.

**pH.** Experiments were performed at pH ranging

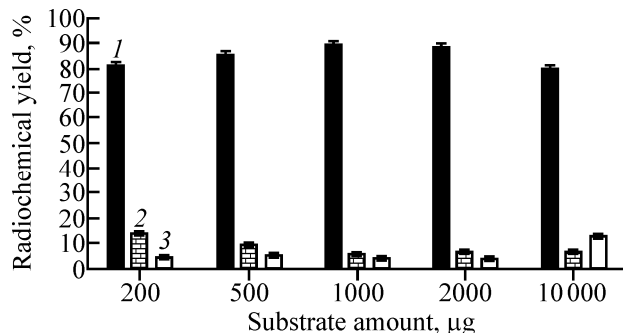


**Fig. 4.** Influence of the KH16 amount on the radiochemical yield of  $^{99m}\text{Tc}$ -KH16. Conditions: 50  $\mu\text{g}$  of Sn(II),  $20\text{mCi mL}^{-1}$   $^{99m}\text{TcO}_4^-$  solution, pH 5, room temperature, 10 min.

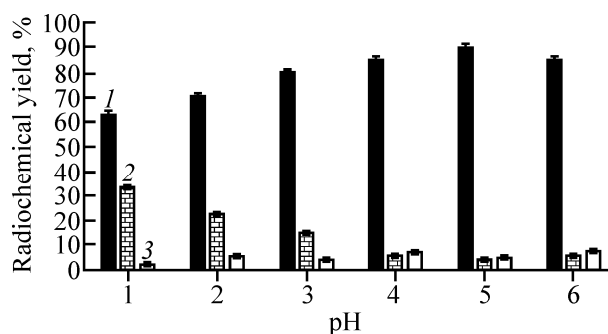


**Fig. 5.** Influence of pH of the reaction medium on the radiochemical yield of  $^{99m}\text{Tc}$ -KH16. Conditions: 1 mg of KH16, 50  $\mu\text{g}$  of Sn(II),  $20\text{mCi mL}^{-1}$   $^{99m}\text{TcO}_4^-$  solution, room temperature, 10 min.

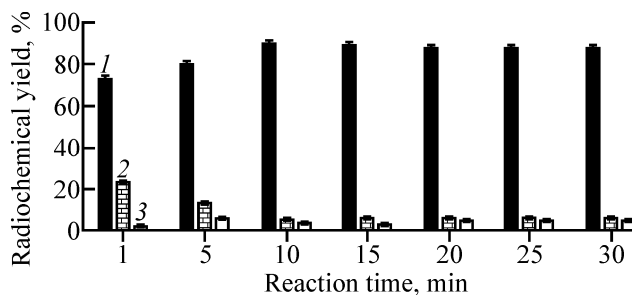


**Fig. 6.** Influence of reaction time on the radiochemical yield of  $^{99m}\text{Tc}$ -KH16. Conditions: 1 mg of KH16, 50  $\mu\text{g}$  of Sn(II),  $20\text{mCi mL}^{-1}$   $^{99m}\text{TcO}_4^-$  solution, pH 5, room temperature.

from 1 to 6 (Fig. 5) with 1 mg of KH16 and 0.5 mL of each buffer. The reaction time was 30 min. pH 5 is optimum (90.5%). At pH > 7, the compound precipitated.

**Reaction time.** The relationship between the reaction time and the yield of  $^{99m}\text{Tc}$ -KH16 is shown in Fig. 6. The radiochemical yield was increased from 73.5 to 90.5% with increasing reaction time from 1 to

**Table 2.** Stability of  $^{99m}\text{Tc}$ -KH16 (relative content, %) in normal saline and human serum ( $n = 3$ )<sup>a</sup>

Time, h	In saline	In human serum
1	91.5 ± 1.7	90.5 ± 1.3
2	90.7 ± 1.3	89.7 ± 1.2
4	90.5 ± 1.5	89.5 ± 1.4
6	85.3 ± 1.9*	83.3 ± 1.7*
8	75.5 ± 1.2*	73.5 ± 1.3*

<sup>a</sup> Here and in Tables 3–5, the values significantly differing from the previous value ( $P < 0.05$ ) are marked with an asterisk.

10 min. Extending the reaction time to 120 min led to a slight decrease in the radiochemical yield [38].

#### *In vitro* Stability of $^{99m}\text{Tc}$ -KH16

As shown in Table 2, incubation of the solution containing  $^{99m}\text{Tc}$ -KH16 for 8 h at 37°C in saline and human serum (five experiments in each case) resulted in a small release of the radioactivity from  $^{99m}\text{Tc}$ -KH16, as determined by paper chromatography. The relative content of  $^{99m}\text{Tc}$ -KH16 decreased in 8 h from 91.5 to 75.5% and from 90.5 to 73.5%, respectively. The complex is practically stable for 4 h.

#### *Biodistribution* of $^{99m}\text{Tc}$ -KH16

**Normal mice.** The data on the  $^{99m}\text{Tc}$ -KH16 biodistribution in normal mice are given in Table 3.  $^{99m}\text{Tc}$ -KH16 was rapidly (in 5 min after injection) distributed in blood, kidneys, heart, liver, and urine. After 30 min, the  $^{99m}\text{Tc}$ -KH16 uptake significantly decreased in blood and heart but increased in kidneys and stomach. At 2 h post injection, the majority of tissues and organs

showed a significant decrease in the  $^{99m}\text{Tc}$ -KH16 uptake.

**Bacterially infected mice.** The  $^{99m}\text{Tc}$ -KH16 biodistribution in bacterially inflamed mice (Table 4) was, on the whole, similar to that in normal mice. The uptake in the bacterially inflamed leg only slightly exceeded that in the normal leg. Thus, the complex is not specific to bacterial infections.

**Sterile inflamed mice.** The  $^{99m}\text{Tc}$ -KH16 biodistribution in sterile inflamed mice (Table 5) is also, on the whole, similar to that in normal mice, but the uptake in the sterile inflamed muscle considerably exceeded that in the normal and infected muscles. Thus,  $^{99m}\text{Tc}$ -KH16 can be used as a model to distinguish between sterile and bacterial inflammations.

#### *Docking Study*

The degree of recognition for KH16 at binding pockets of the COX-1 and COX-2 enzymes was evaluated using Molecular Operating Environment 10.2008 (MOE) software (Chemical Computing Group, Canada). The calculation results (Fig. 7) show that KH16 exhibits affinity for the amino acid residues of COX-2 pocket, namely, Phe518 and Ala527. Strong hydrogen bonds are formed between the ester carbonyl oxygen and Phe518 at the end cleft of the merged pocket and the free Ala527 amino group at the terminal end of the groove.

On the other hand, KH16 was poorly recognized at the narrow binding pocket, as it formed only one hydrogen bond with Tyr355; therefore, the ability to inhibit COX-1 is lower.

**Table 3.** Biodistribution of  $^{99m}\text{Tc}$ -KH16 in normal mice (% ID/g ± SD,  $n = 5$ ) at different times post injection

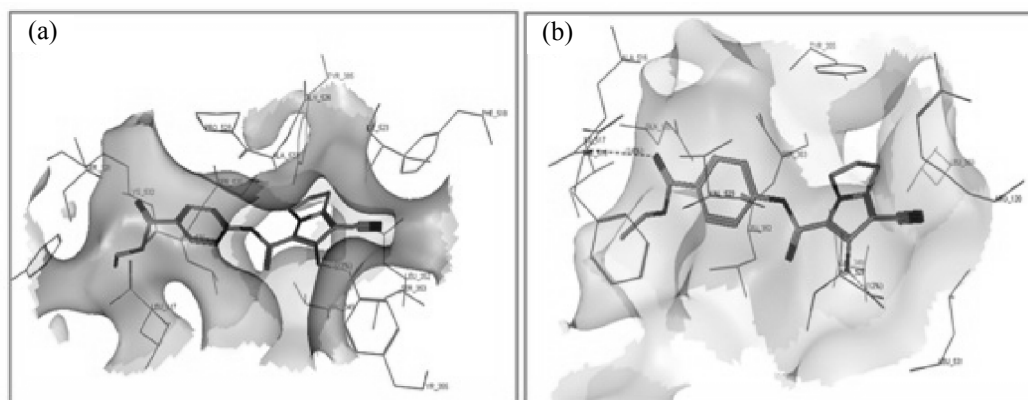
Organs and body fluids	5 min	15 min	30 min	60 min	120 min
Blood	15.50 ± 0.14	13.80 ± 0.23*	7.10 ± 0.18*	4.70 ± 0.01*	1.50 ± 0.02*
Bones	1.20 ± 0.01	1.60 ± 0.01*	1.41 ± 0.03	1.10 ± 0.01*	0.88 ± 0.02*
Muscles	1.20 ± 0.01	1.50 ± 0.03*	1.80 ± 0.04*	1.90 ± 0.01	1.30 ± 0.01*
Brain	0.40 ± 0.01	0.90 ± 0.02*	1.23 ± 0.03*	0.60 ± 0.01*	0.50 ± 0.03
Lungs	1.70 ± 0.01	1.90 ± 0.02*	2.40 ± 0.03*	1.70 ± 0.03*	0.90 ± 0.02*
Heart	4.5 ± 0.5	3.50 ± 0.11*	3.1 ± 0.3	2.7 ± 0.4	1.80 ± 0.15*
Liver	3.30 ± 0.14	4.10 ± 0.18*	3.40 ± 0.24*	3.11 ± 0.11	1.20 ± 0.11*
Kidneys	5.28 ± 0.16	6.90 ± 0.41*	6.11 ± 0.02	12.50 ± 0.18*	18.0 ± 0.13*
Spleen	1.10 ± 0.01	1.70 ± 0.01*	2.30 ± 0.22*	0.95 ± 0.03*	0.70 ± 0.01*
Intestine	1.90 ± 0.01	3.90 ± 0.22*	4.90 ± 0.01*	5.40 ± 0.01*	3.50 ± 0.15*
Stomach	1.10 ± 0.01	3.95 ± 0.03*	4.80 ± 0.01*	3.85 ± 0.01*	3.80 ± 0.02
Thyroid	0.95 ± 0.01	0.70 ± 0.02*	0.80 ± 0.01	1.10 ± 0.03	1.11 ± 0.01

**Table 4.** Biodistribution of  $^{99m}\text{Tc}$ -KH16 in bacterially infected mice (% ID/g  $\pm$  SD,  $n = 5$ ) at different times post injection

Organs and body fluids	5 min	15 min	30 min	60 min	120 min
Blood	14.90 $\pm$ 0.11	12.6 $\pm$ 0.23*	11.2 $\pm$ 0.18*	5.50 $\pm$ 0.01*	2.40 $\pm$ 0.02*
Bones	1.20 $\pm$ 0.01	1.70 $\pm$ 0.01*	1.60 $\pm$ 0.03	1.30 $\pm$ 0.01*	0.90 $\pm$ 0.02*
Brain	0.30 $\pm$ 0.01	0.80 $\pm$ 0.02*	1.20 $\pm$ 0.03*	0.60 $\pm$ 0.01*	0.65 $\pm$ 0.03
Lungs	1.60 $\pm$ 0.01	1.70 $\pm$ 0.02	2.30 $\pm$ 0.03*	2.80 $\pm$ 0.03*	1.90 $\pm$ 0.02*
Heart	4.1 $\pm$ 0.5	3.50 $\pm$ 0.11*	3.1 $\pm$ 0.3	2.7 $\pm$ 0.4	1.80 $\pm$ 0.15*
Liver	4.30 $\pm$ 0.14	4.40 $\pm$ 0.18	4.40 $\pm$ 0.24	3.40 $\pm$ 0.11*	1.30 $\pm$ 0.11*
Kidneys	5.60 $\pm$ 0.16	6.7 $\pm$ 0.4*	6.40 $\pm$ 0.02	10.90 $\pm$ 0.18*	16.8 $\pm$ 1.3*
Spleen	1.13 $\pm$ 0.01	1.80 $\pm$ 0.01*	2.40 $\pm$ 0.22*	0.85 $\pm$ 0.03*	0.40 $\pm$ 0.01*
Intestine	1.85 $\pm$ 0.01	3.50 $\pm$ 0.22*	4.20 $\pm$ 0.01*	5.10 $\pm$ 0.01*	3.90 $\pm$ 0.15*
Stomach	0.95 $\pm$ 0.01	2.95 $\pm$ 0.03*	3.80 $\pm$ 0.01*	3.65 $\pm$ 0.01*	3.30 $\pm$ 0.02*
Thyroid	0.95 $\pm$ 0.01	0.77 $\pm$ 0.02*	0.85 $\pm$ 0.01*	1.10 $\pm$ 0.03*	1.14 $\pm$ 0.01
Normal muscle	1.30 $\pm$ 0.01	1.30 $\pm$ 0.01	1.20 $\pm$ 0.01	1.30 $\pm$ 0.01	1.20 $\pm$ 0.01
Infected muscle	1.50 $\pm$ 0.25	1.6 $\pm$ 0.3	1.7 $\pm$ 0.3	1.40 $\pm$ 0.20	1.3 $\pm$ 0.3

**Table 5.** Biodistribution of  $^{99m}\text{Tc}$ -KH16 in sterile inflamed mice (% ID/g  $\pm$  SD,  $n = 5$ ) at different times post injection

Organs and body fluids	5 min	15 min	30 min	60 min	120 min
Blood	14.5 $\pm$ 0.11	12.8 $\pm$ 0.23*	11.1 $\pm$ 0.18*	5.70 $\pm$ 0.01*	2.50 $\pm$ 0.02*
Bones	1.10 $\pm$ 0.01	1.50 $\pm$ 0.01*	1.60 $\pm$ 0.03	1.20 $\pm$ 0.01*	0.80 $\pm$ 0.02*
Brain	0.35 $\pm$ 0.01	0.75 $\pm$ 0.02*	1.10 $\pm$ 0.03*	0.70 $\pm$ 0.01*	0.65 $\pm$ 0.03
Lungs	1.50 $\pm$ 0.01	1.60 $\pm$ 0.02	2.20 $\pm$ 0.03*	2.60 $\pm$ 0.03*	2.10 $\pm$ 0.02*
Heart	3.8 $\pm$ 0.5	3.60 $\pm$ 0.11	2.90 $\pm$ 0.33*	2.70 $\pm$ 0.44	1.70 $\pm$ 0.15*
Liver	4.50 $\pm$ 0.14	4.60 $\pm$ 0.18	4.60 $\pm$ 0.24	3.30 $\pm$ 0.11*	1.30 $\pm$ 0.11*
Kidneys	5.40 $\pm$ 0.16	6.10 $\pm$ 0.4*	5.95 $\pm$ 0.02	11.80 $\pm$ 0.18*	15.80 $\pm$ 0.30*
Spleen	1.10 $\pm$ 0.01	1.60 $\pm$ 0.01*	2.20 $\pm$ 0.22*	0.95 $\pm$ 0.03*	0.60 $\pm$ 0.01*
Intestine	1.80 $\pm$ 0.01	3.60 $\pm$ 0.22*	4.50 $\pm$ 0.01*	5.20 $\pm$ 0.01*	3.90 $\pm$ 0.15*
Stomach	1.05 $\pm$ 0.01	3.80 $\pm$ 0.03*	4.60 $\pm$ 0.01*	3.65 $\pm$ 0.01*	3.70 $\pm$ 0.02
Thyroid	0.93 $\pm$ 0.01	0.72 $\pm$ 0.02*	0.83 $\pm$ 0.01	1.10 $\pm$ 0.03*	1.13 $\pm$ 0.01
Normal muscle	1.30 $\pm$ 0.01	1.30 $\pm$ 0.01	1.20 $\pm$ 0.01	1.30 $\pm$ 0.01	1.20 $\pm$ 0.01
Inflamed muscle	2.5 $\pm$ 0.4	5.6 $\pm$ 0.5*	6.10 $\pm$ 0.51	5.20 $\pm$ 0.51	4.30 $\pm$ 0.51
T/NT	1.92 $\pm$ 0.3	4.3 $\pm$ 0.4	5.08 $\pm$ 0.40	4.0 $\pm$ 0.20	3.58 $\pm$ 0.30

**Fig. 7.** Docking of KH16 in the active sites of (a) COX-1 (one H-bond between  $\text{NH}_2$  and Tyr355) and (b) COX-2 (two H-bonds between ester carbonyl oxygen and  $\text{NH}_2$  of Phe518 and Ala527).

Thus, KH16 demonstrated good inhibitory activity for COX-1 and COX-2 enzymes with IC<sub>50</sub> values of 5.33 and 1.54 μM, respectively (selectivity index 3.46). A docking study revealed the formation of two H-bonds between KH16 and amino acid residues in COX-2, whereas only one H-bond is formed with the active site of COX-1 enzyme. KH16 was labeled with <sup>99m</sup>Tc with a yield of about 90%. The labeled compound allows revealing sterile inflammation but is practically nonspecific to bacterial inflammation. KH16 is a promising scaffold for the development of potential anti-inflammatory agents.

#### ACKNOWLEDGMENTS

The authors are grateful to the Institute of Scientific Research and Revival of Islamic Heritage, Umm Al-Qura University, Makkah, Saudi Arabia, for financial support of the study (project no. 43310014).

#### REFERENCES

1. Roberts, L.J. and Morrow, J.D., *The Pharmacological Basis of Therapeutics*, Goodman, L.S., Gilman, A.G., Hardman, J.G., and Limbird, A.E., Eds., New York: McGraw-Hill, 2001, 10th ed., pp. 687–733.
2. Schneider, V., Levesque, L.E., Zhang, B., et al., *Am. J. Epidemiol.*, 2006, vol. 164, pp. 881–889.
3. Cryer, B., *Am. J. Gastroenterol.*, 2005, vol. 100, pp. 1694–1695.
4. Singh, G., *Am. J. Med.*, 1998, vol. 105, pp. 31S–38S.
5. Vane, J.R. and Botting, R.M., *Scand. J. Rheumatol. Suppl.*, 1996, vol. 102, pp. 9–21.
6. Smith, C.J., Zhang, Y., Koboldt, C.M., et al., *Proc. Nat. Acad. Sci.*, 1998, vol. 95, pp. 133–138.
7. Sarkar, F.H., Adsule, S., Li, Y., and Padhye, S., *Mini Rev. Med. Chem.*, 2007, vol. 7, pp. 599–608.
8. Gouda, A.M. and Abdelazeem, A.H., *Eur. J. Med. Chem.*, 2016, vol. 114, pp. 257–292.
9. Laufer, S.A., Augustin, J., Dannhardt, G., and Kiefer, W., *J. Med. Chem.*, 1994, vol. 37, pp. 1894–1897.
10. Bias, P., Buchner, A., Klessner, B., and Laufer, S., *Am. J. Gastroenterol.*, 2004, vol. 99, pp. 611–618.
11. Ulbrich, H., Fiebich, B., and Dannhardt, G., *Eur. J. Med. Chem.*, 2002, vol. 37, pp. 953–959.
12. Laufer, S., Tollmann, K., and Striegel, H.G., US Patent 6 878 738 B1, 2005.
13. Liu, W., Zhou, J., Bensdorf, K., et al., *Eur. J. Med. Chem.*, 2011, vol. 46, pp. 907–913.
14. Liedtke, A.J., Keck, P.R., Lehmann, F., et al., *J. Med. Chem.*, 2009, vol. 52, pp. 4968–4972.
15. Jett, M.F., Ramesha, C.S., Brown, C.D., et al., *J. Pharmacol. Exp. Ther.*, 1999, vol. 288, pp. 1288–1297.
16. Guzman, A., Yuste, F., Toscano, R.A., et al., *J. Med. Chem.*, 1986, vol. 29, pp. 589–591.
17. Simone, O.F.D., Cristiano, F.S., David, L.N., et al., *Braz. Arch. Boil. Technol.*, 2005, vol. 48, pp. 89–96.
18. Beiki, D., Yousefi, G., Fallahi, B., et al., *Iran. J. Pharm. Res.*, 2013, vol. 12, pp. 347–353.
19. Sanad, M.H. and Amin, A.M., *Radiochemistry*, 2013, vol. 55, no. 5, pp. 521–526.
20. Oliveira Pereira, M., Souza Rocha, G., Medeiros, A.C., et al., *Med. Chem. Res.*, 2011, vol. 21, pp. 1433–1438.
21. El-Ghany, E.A., Amin, A.M., El-Kawy, O.A., and Amin, M., *J. Label. Compd. Radiopharm.*, 2007, vol. 50, pp. 25–31.
22. Welling, M.M., Lupetti, A., Balter, H.S., et al., *J. Nucl. Med.*, 2001, vol. 42, pp. 788–794.
23. Abbas, S.E., Awadallah, F.M., Ibrahim, N.A., and Gouda, A.M., *Eur. J. Med. Chem.*, 2010, vol. 45, pp. 482–491.
24. Etienne, A. and Correia, Y., *Bull. Soc. Chim. Fr.*, 1969, vol. 10, pp. 3704–3712.
25. Jacobs, W.A. and Heidelberger, M., *J. Am. Chem. Soc.*, 1917, vol. 39, pp. 1435–1439.
26. Praveen Rao, P.N., Amini, M., Li, H., et al., *J. Med. Chem.*, 2003, vol. 46, pp. 4872–4882.
27. Motaleb, M.A., El-Said, H., Atef, M., and Abd-Allah, M., *Radiochemistry*, 2012, vol. 54, no. 3, pp. 274–278.
28. Moustapha, M.E., Motaleb, M.A., and Ibrahim, I.T., *J. Radioanal. Nucl. Chem.*, 2011, vol. 287, pp. 35–40.
29. Van Der Laken, C.J., Boerman, O.C., and Oyen, W.J.G., *J. Nucl. Med.*, 2000, vol. 41, pp. 463–469.
30. Oyen, W.J.G., Boerman, O.C., and Corstens, F.H.M., *J. Microbiol. Meth.*, 2001, vol. 47, pp. 151–157.
31. Asikoglu, M., Yurt, F., Cagliyan, O., et al., *Appl. Radiat. Isot.*, 2000, vol. 53, pp. 411–413.
32. Johannsen, B. and Spies, H., Chemistry and radiopharmacology of technetium complexes, *Workshop on Generator and Cyclotron Produced Radiopharmaceuticals*, Riyadh (Saudi Arabia), Oct. 13–31, 1991.
33. Sanad, M.H., Borai, E.H., and Fawzy, A.S.M., *IOSR J. Environ. Sci., Toxicol. Food Technol.*, 2014, vol. 8, pp. 10–17.
34. Kurumbail, R.G., Stevens, A.M., Gierse, J.K., et al., *Nature*, 1996, vol. 384, pp. 644–648.
35. Harman, C.A., Turman, M.V., Kozak, K.R., et al., *J. Biol. Chem.*, 2007, vol. 282, pp. 28096–28105.
36. Warner, T.D., Giuliano, F., Vojnovic, I., et al., *Proc. Natl. Acad. Sci. USA*, 1999, vol. 96, pp. 7563–7568.
37. Sankha, C., Sujata, S.D., Susmita, C., et al., *Appl. Radiat. Isot.*, 2010, vol. 68, pp. 314–316.
38. Sarda, L., Cremieux, A.C., Lebellec, Y., et al., *J. Nucl. Med.*, 2003, vol. 44, pp. 920–926.